sciendo

Civil and Environmental Engineering
Vol. 19, Issue 2, 543-554, DOI: 10.2478/cee-2023-0049

TENSILE FORCE DISTRIBUTION AND DEVELOPMENT WITHIN GEOGRID-REINFORCED RETAINING WALL

Marwa FELIGHA[1,*], Fatima Zohra BENAMARA[2], Nouaouria Mohamed SALAH[2], Souhila Rehab BEKKOUCHE[1], Benayoun FADILA[3]

[1] University 20 Aout 1955, Department of Civil Engineering, LMGHU Laboratory, Skikda, Algeria.
[2] University 8 May 1945, Department of Civil Engineering and Hydraulics, LGCH Laboratory, Guelma, Algeria.
[3] University of Larbi Ben M'hidi, Department of Civil Engineering, LDDPE Laboratory, Oum El Bouaghi, Algeria.
[*] corresponding author: feligha_marwa@yahoo.com

Abstract

Geogrid-reinforced earth retaining walls used to improve soil quality, and provide additional shear strength in the soil mass through the tensile strength in the reinforcement layers. A numerical model was developed by finite element code PLAXIS2D, of a segmental facing geogrid-reinforced retaining wall. This research has been carried out to investigate the effect of loading increments, loading increments width, loading increments location, facing inclination angle, geogrid inclination angle, and geogrid-soil friction factor, on the behaviour of a geogrid-reinforced soil retaining wall. The results show that the failure plane occurred in the reinforced zone at the mid-height, this observation contradicted the triangular distribution with depth assumed in conception methodologies for reinforced soil retaining wall. The distribution of peak tensile strength with depth was bilinear at high loading increments and became trapezoidal at low loading ones. Furthermore, it was found that the behaviour of a geogrid-reinforced soil retaining wall is independent of loading increments width beyond 0.5*H*. It also seems that the loading increments location can change the shape and the position of the peak tensile strength. It also seems that the geogrid inclination angle has a major effect on the lateral facing displacements and safety factor.

Keywords:

Failure surface;
Lateral displacement;
PLAXIS[2D];
Retaining wall;
Tensile strength.

1 Introduction

Geogrid-reinforced soil retaining wall has been developed for a wide variety of applications in several fields (geotechnics, hydraulics, mechanics, engineering etc.). This latter was a composite structure formed by soil-geogrid interaction. The main function of the geogrid layers was to improve the tensile strength of soil. Reinforced soil retaining wall was calculated using the conception method of American Association of State Highway and Transportation Officials (AASHTO [1]), which were based on the limit equilibrium approach. This conception method neglects several parameters that affect the performance of reinforced soil retaining walls.

[2] performed numerical simulations using the finite element program AFENA to study the influence of several geometrical and mechanical parameters on the behavior of the reinforced retaining wall, postulating that the most important factors affecting the peak tensile strength were: reinforcement stiffness density; facing-soil friction factor; soil friction angle; and facing rigidity.

[3] used the two-dimensional, explicit finite difference program (FLAC) to perform the numerical experiments. They indicated that the results of the lateral facing displacement and the peak tensile strength of the reinforcement are in agreement with the results of [4].

To study the effect of loading increments, [5] performed full-scale tests to validate double block method, based on the limit equilibrium approach, consists of locating the failure surfaces to calculate

© Author(s) 2023. This work is distributed under the Creative Commons BY 4.0 license (https://creativecommons.org/licenses/by/4.0/).

the peak tensile strength and the safety factor. He showed that this method gives a conservative solution in several cases.

[6] carried out a numerical research of a geosynthetic reinforced soil walls, using the FLAC^{2D} (Fast Lagrangian Analysis of Continua). The numerical results show that peak tensile strength in the reinforcement layers and lateral displacement of the facing increase with increasing uniform loading increments.

The numerical analysis to study the influence of facing inclination angle was examined by [7]. The results show that the peak tensile strength decreases with increasing facing inclination angle.

In order to examine the behavior of geosynthetic reinforced soil retaining wall, [8] used the PLAXIS^{2D} finite element code. The comparison of numerical and experimental results show that predicts peak tensile strength in the reinforcement layers at the end of construction were closer to the measured values.

The width and position of loading are one factor that changes the response of reinforced retaining wall, have been the subject of experimental and numerical works [6, 9-11].

[12] studied the design of geogrid reinforced road embankments with a passive facing system. Analytical calculations were performed using the geotechnical software fine Geo5 and numerical modeling was performed using the software Plaxis^{2D}. The results of the study showed that numerical modeling is more appropriate for geogrid reinforced road supported embankment wrapped design with the passive facing system because it allowed for more accurate complex boundary conditions.

The present paper aims to evaluate the influence of loading increments, loading increments width, loading increments location, facing inclination angle, geogrid inclination angle, and geogrid-soil friction factor on the behaviour of a geogrid-reinforced soil retaining wall to analyze peak tensile strength, lateral facing displacements, critical failure surfaces and safety factor, using the PLAXIS^{2D} code [13].

2 Models for mechanical failure

The stability conditions of geogrid-reinforced soil retaining walls are influenced by the geometry, the soil mechanical properties, and soil-reinforcement interaction mechanism. The principle of failure detection can be summarized in two steps:

• the objective of the first step is to identify the geometrical configurations favorable to failure for the different known failure mechanisms;

• the second step involves the calculation of the safety factors associated with each failure mechanism identified in the previous step.

We assume that the critical failure surface of a reinforced earth wall coincides with the line of peak tensile strength, i.e. the critical failure surface located according to the points of peak tensile strength in each reinforcement layer, Fig.1.

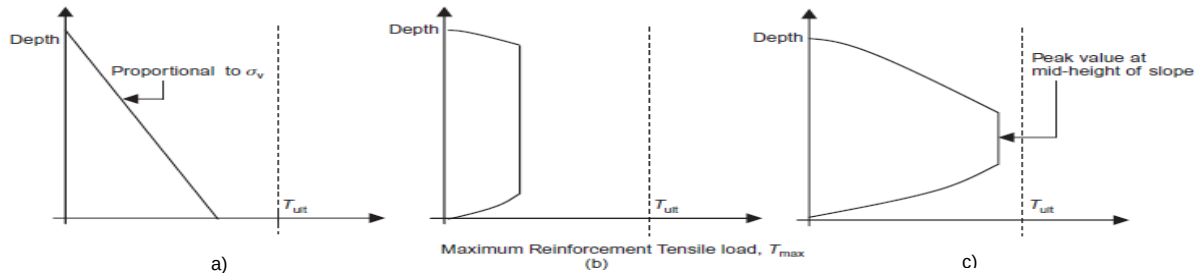


Fig. 1: Location of tensile strength reinforced soil retaining walls: a) design methodologies for geosynthetic walls; b) uniform distribution for low loading increments; c) trapezoidal distribution for high loading increments [14].

3 Numerical model

3.1 Reference case definition

The reference case was 6 m high and 13 m long from the facing, Fig. 2, with a segmental facing of thickness 0.14 m. The geogrid layers placed horizontally with a length of 4.25 m which is around to 0.7*H* to meet the AASHTO conception method [1], and spaced 1 m apart vertically. Also, the building phasing was respected. The geometry of the model examined in this paper was shown in Fig. 2. The

plane deformation behavior of this wall was simulated by [3] using the FLAC code, based on the finite difference method.

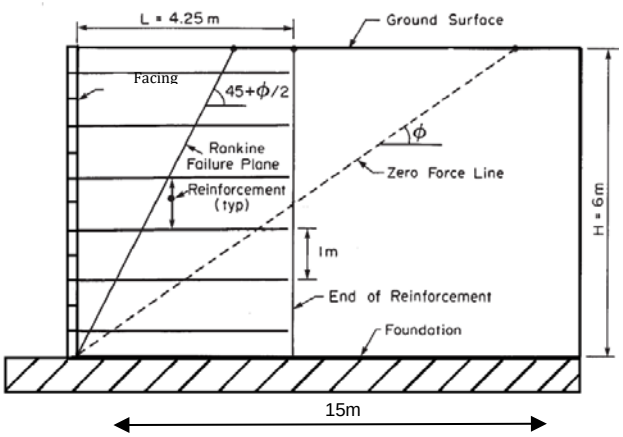
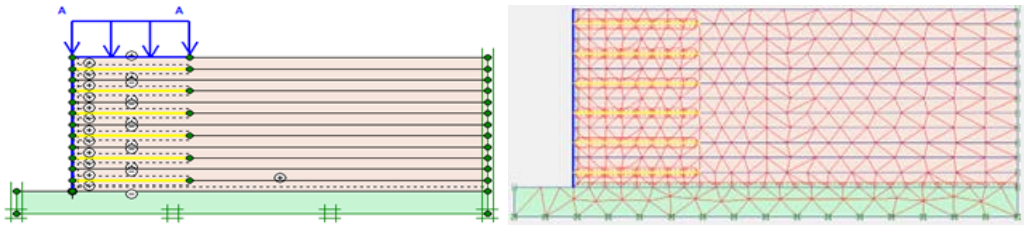


Fig. 2: Geometry of numerical reference model [4].

Fig. 3 shows the numerical model used in this investigation. The elastic perfectly plastic model with Mohr-Coulomb criterion was adopted to model the reinforced and unreinforced soil; moreover, the facing was modeled by a three-node beam elements called "plate" in PLAXIS^{2D} code [13]. The foundation was assumed to be rigid and has a unit weight of 23 kN/m^3, its behavior was governed by linear elastic criterion. The soil-geogrid, soil-foundation and soil-facing contact was modeled by a rigid interface element with an interface friction angle of 20°. The reinforcement layers were simulated using six geogrid elements that are available in PLXIS^{2D}, the axial stiffness was taken as *EA* = 2000 kN/m. This latter was chosen with linear elastic behavior and the creep phenomenon is neglected. The materials properties were estimated from the studies performed by [3] as summarized in Table 1.



a) b)

Fig. 3: Numerical model a) Cross-sectional view. b) Meshes for the reference case.

Table 1: Soil reinforcement and facing properties.

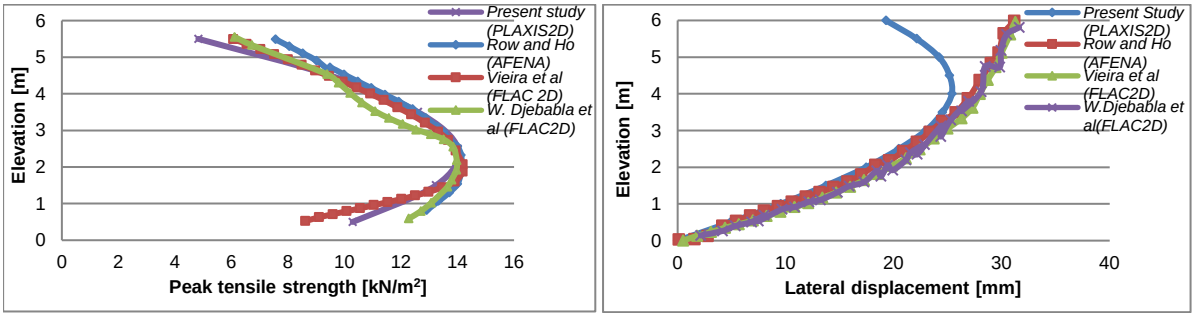
Soil reinforcement	ν	Poisson's coefficient	0.3
	Ψ	Dilatancy angle [°]	5
	φ	Friction angle [°]	35
	c	Cohesion [kPa]	1
	E	Young's modulus [kN/m^2]	$3.5 \cdot 10^4$
	γ	Unit weight [kN/m^3]	20
	δ	Interface soil-facing friction angle [°]	20
Facing	EA	Normal stiffness [kN/m]	$5 \cdot 10^6$
	EI	Flexural rigidity [kN·m^2/m]	$8.5 \cdot 10^3$

3.2 Validation of the numerical model

In the first stage of this study, a series of analyses was performed to validate our model and for the parametric study to be reliable. The numerical model, reported by [4], have been considered by several researchers such as [3, 6, 15]. These results were also used to validate the numerical model developed in this study, because it presents a good characterization of the materials and a good construction sequence.

Fig. 4a illustrates the peak tensile strength results under the self-weight of reinforced soil adopted in the present study and compared with those of [4, 6, 15]. It can be seen that the numerical results of the peak tensile strength were in good agreement with those of the above authors.

Fig. 4b presents lateral facing displacement. It seems to be in accordance with the results obtained by the above-mentioned authors. With exception at the third upper part of the wall, the lateral displacement decreases. The difference may be due to the treatment with the segmental facing panel. The maximum lateral displacement obtained for this case was about 25.72 mm which presents a strain of about 4.73 % located at the interface between the reinforced soil and the facing.



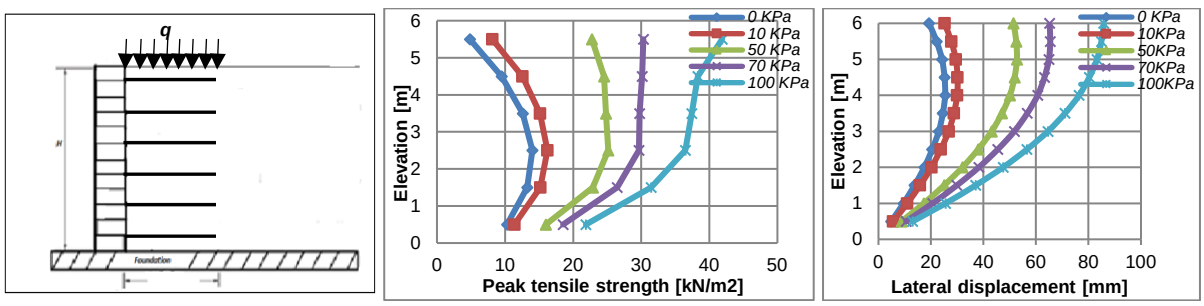
a) b)

Fig. 4: Comparison results a) Peak tensile strength. b) Lateral facing displacement.

3.3 Effect of loading increments *q*

The effect of loading increments ranging from 0 kPa, 10 kPa, 50 kPa, 70 kPa, and 100 kPa, on the peak tensile strength and the lateral facing displacement is illustrated in Fig. 5b, c.

According to the results obtained, we notice an increase of the peak tensile strength in the geogrid layers with the increase of loading increments. A trapezoidal shape of peak tensile strength with depth at low loading increments q < 50 kPa, with the critical value was located at a height of 0.5H above the base of wall. This value seems to agree with the results obtained in the bibliographical research. [14] conducted numerically by finite element method a series of centrifuge tests on two reinforced soil retaining slopes. They postulated that the peak value of tensile strength was positioned approximately halfway up the reinforced slopes. Furthermore, [16] carried out scale models with digital image analysis to evaluate the deformation distribution in the geosynthetic reinforced soil. They founded that the location of critical deformation of the reinforcement was not at the base of the slope, but was approximately located at mid-height of the slope. The distribution of the peak tensile strength at high loading increments q > 50 kPa depicts a bilinear distribution, It was noted that similar results were reported by [17]. The distribution of peak tensile strength in the current study does not follow the triangular distribution with depth assumed in geogrid-reinforced retaining wall conception methodologies. It can be observed that the lateral displacement increases with increasing loading increments.



a) b) c)

Fig. 5: a) Position of loading increments. b) Effect of loading increments on peak tensile strength. c) Effect of loading increments on lateral facing displacement.

The calculation of the safety factor F_s in PLAXIS^{2D} [13] can be done by reduction of strength parameters c and tanϕ until failure is achieved. This process is called "Phi-C reduction" and resembles the safety factor calculation method conventionally adopted in sliding critical failure surfaces. The

incremental multiplier ΣM_{sf} used to define the value of the soil characteristics at a given stage of the analysis equation (1):

$$\sum M_{SF} = \frac{\tan\varphi_{input}}{\tan\varphi_{reduced}} = \frac{c_{input}}{c_{reduced}} \quad (1)$$

Fig. 6 shows that, as loading increments increase from 0 kPa to 100 kPa, the magnitude for the safety factor decreases. Also, it can be seen that the geogrid-reinforced soil retaining wall unstable to loading increments was greater than 90 kPa. The required safety factor for reinforcement stability, recommended by AASHTO (2012) [1], equals to 1.5.

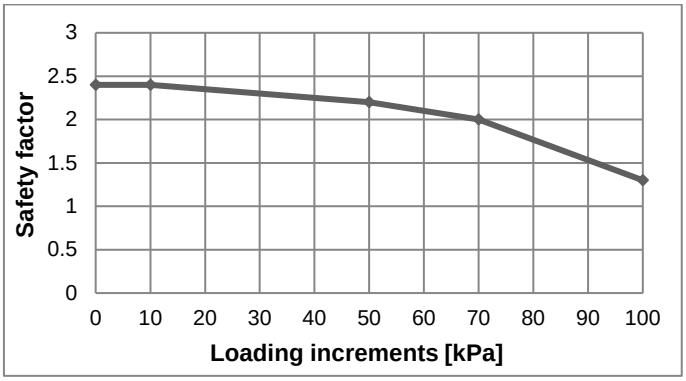


Fig. 6: Safety factor for different loading increments.

3.4 Effect of loading increments width *l*

The evaluation of reinforced soil retaining wall behavior subjected to five different loading increments widths *l* = 1.2m, 2.92 m, 4.25 m, 6 m, and 15 m are summarized in Fig. 7.

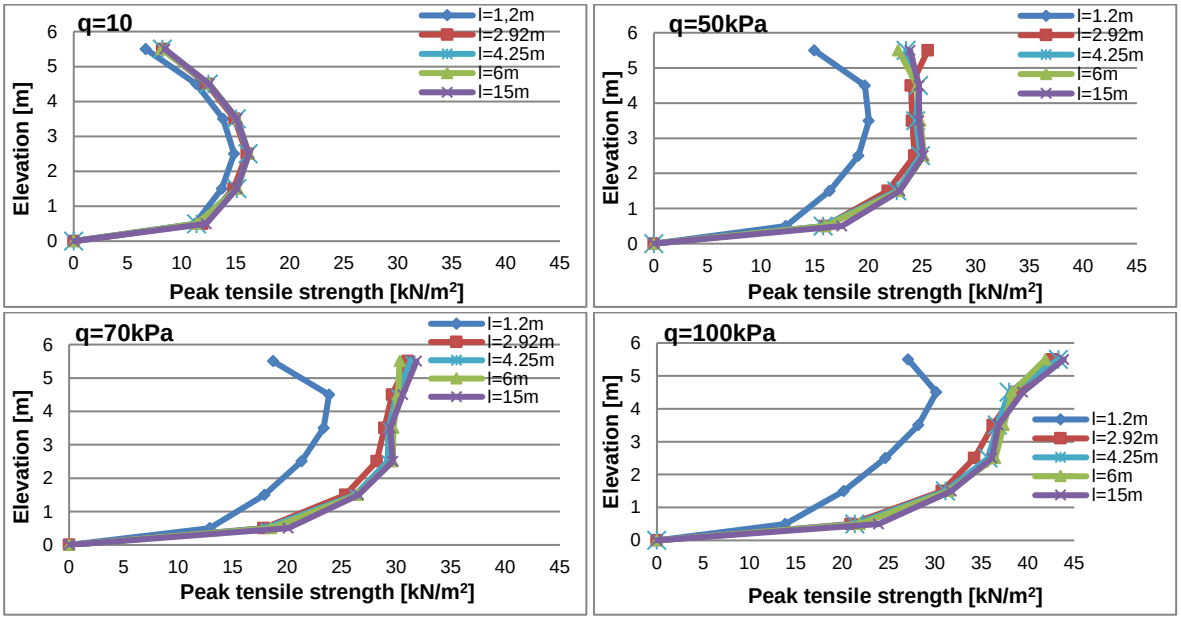


Fig. 7: Effect of different loading increments width on peak tensile strength.

The peak tensile strength increase with increasing of loading increments width, this increase was less important for the lower layers, because of the distribution of loading with depth. The increase of loading increments width beyond 0.5*H* (*l* = 2.92 m) has practically no effect on the distribution of peak tensile strength, which coincides with the Ranking' failure surface. Note that the AASHTO (2012) conception method does not take into account the loading increments applied on the unreinforced soil for the calculation of peak tensile strength (maximum width of 0.7*H*), which leads to an underestimation of the tensile strength of the reinforcement layers. It is noted that similar results reported by [6], show that the width (6m and 8m) of different loading increments applied have no effect on the normalized

peak tensile strength. [10] carried out a numerical study to evaluate the effect of the loading width on the behavior of the reinforced soil retaining walls. Increasing the width of the loading for small height walls H = 3.6 m do not affect the distribution of normalized peak tensile strength while for large height walls H = 6.2 m and H = 12.4 m the normalized peak tensile strength increases with increasing loading width.

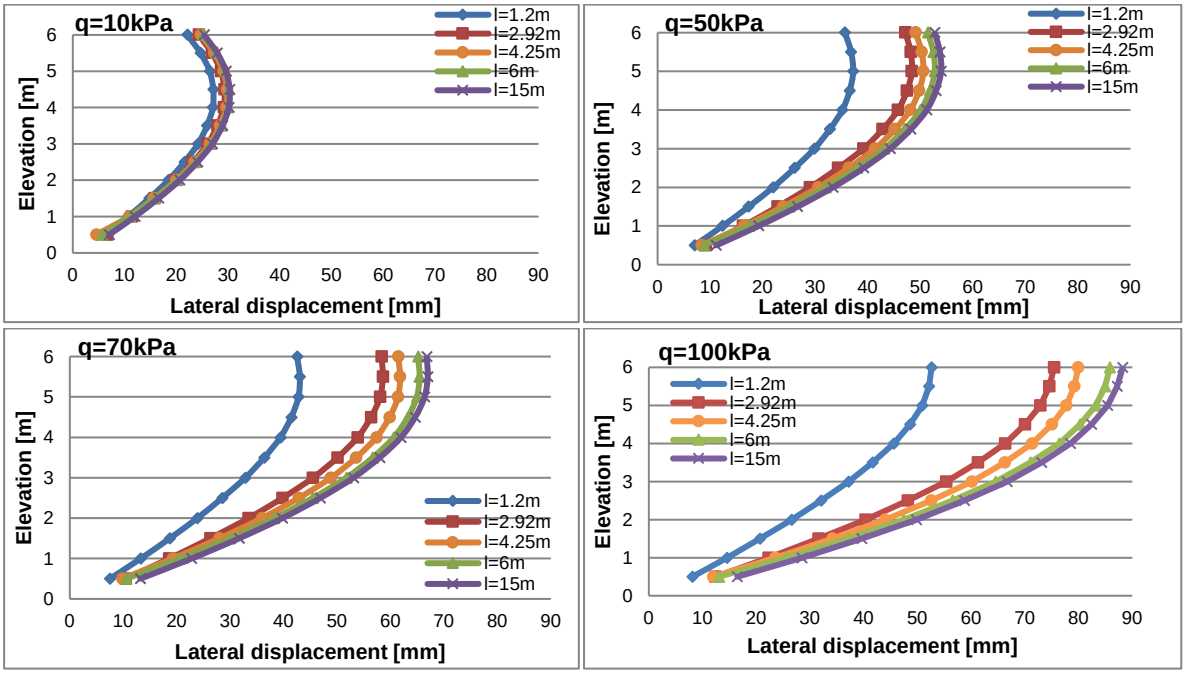


Fig. 8: Effect of different loading increments width on lateral facing displacement.

In order to assess the effect of different loading increments width on the lateral facing displacement, the results are presented in Fig 8. As observed it could be observed that no trend was observed regarding the values of lateral facing displacement which appear not to be affected by the loading increments width beyond 0.5H (l = 2.92 m), regarding low value of q = 10 kPa. For high loading increments q ≥ 50 kPa the lateral facing displacement increases with increasing different loading increments width.

3.5 Effect of loading increments location *s*

The peak tensile strength measured at the geogrid layers for the same loading increment width l = 2.92 m, under different loading increments locations s = 0 m; 1 m; 2 m; 3 m; 4 m, is illustrated in Fig. 9. The comparison of the curves shows that the increase in loading increments locations decreases the peak tensile strength in the geogrid layers. Furthermore, the loading increments location applied for s = 3 m and s = 4 m has no effect on the peak tensile strength. The position of the peak tensile strength mobilized along the geogrid layers depends on the loading increments location conditions, where this latter was transferred from geogrid layer 3 to geogrid layer 2. This phenomenon is more pronounced for the higher loading values. This coincides with the results of the experimental study of [11]. As observed, the same shape (trapezoidal) were obtained for all loading increment locations for q = 10 kPa, while for q > 50 kPa the development of the curves shape changed with the loading increments location, exhibiting a bilinear distribution for s = 0 m to a trapezoidal distribution for other locations s = 1 m, 2 m, 3 m and 4 m. These results highlight the importance of loading increment location for the failure mechanism.

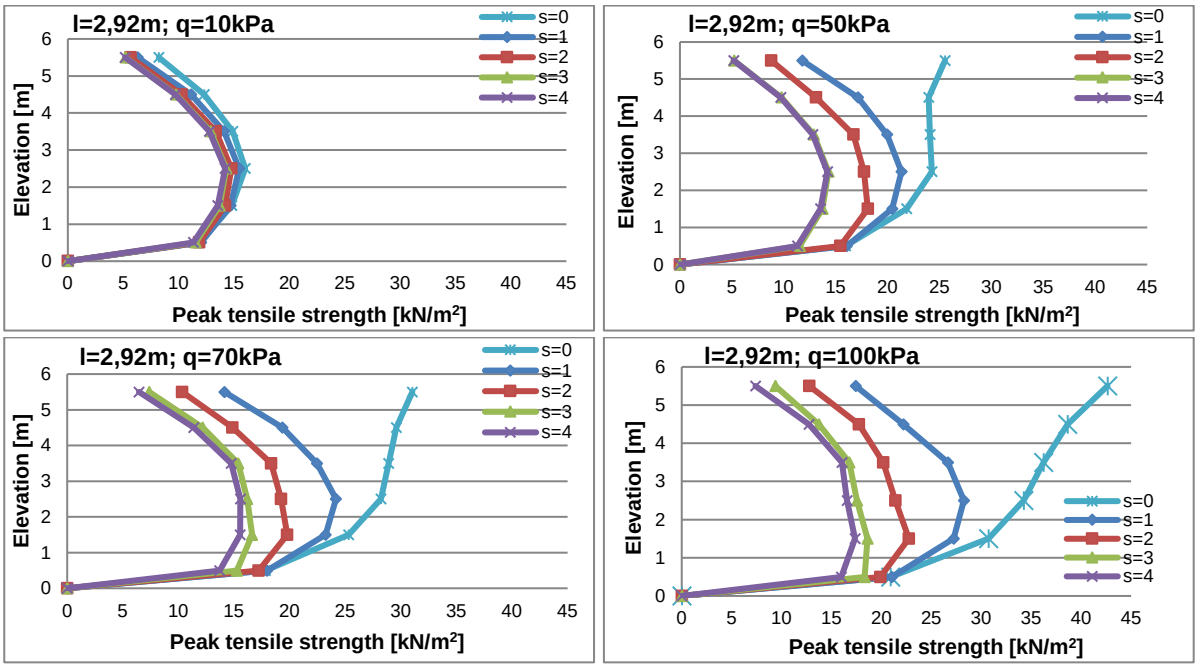


Fig. 9: Effect of different loading increment locations on peak tensile strength.

In order to evaluate the effect of loading locations on the peak tensile strength, the results are also presented in Fig. 10 in the form of column graphs that consist of four categories, each representing a loading location. It shows the peak tensile strength of different loadings increments 10 kPa; 50 kPa; 70 kPa; 100 kPa, with different loading widths l = 1.2 m; 2.92 m; 6 m. It noted that no trend was observed in the values of the peak tensile strength, which seem to be unaffected by the width and the location of low load q = 10 kPa. In addition, it should also be noted that the peak tensile strength decreases with increasing loading location of different widths of applied loading for $q \geq 50$ kPa, except the case where s = 3 m and s = 4 m found approximately the same values.

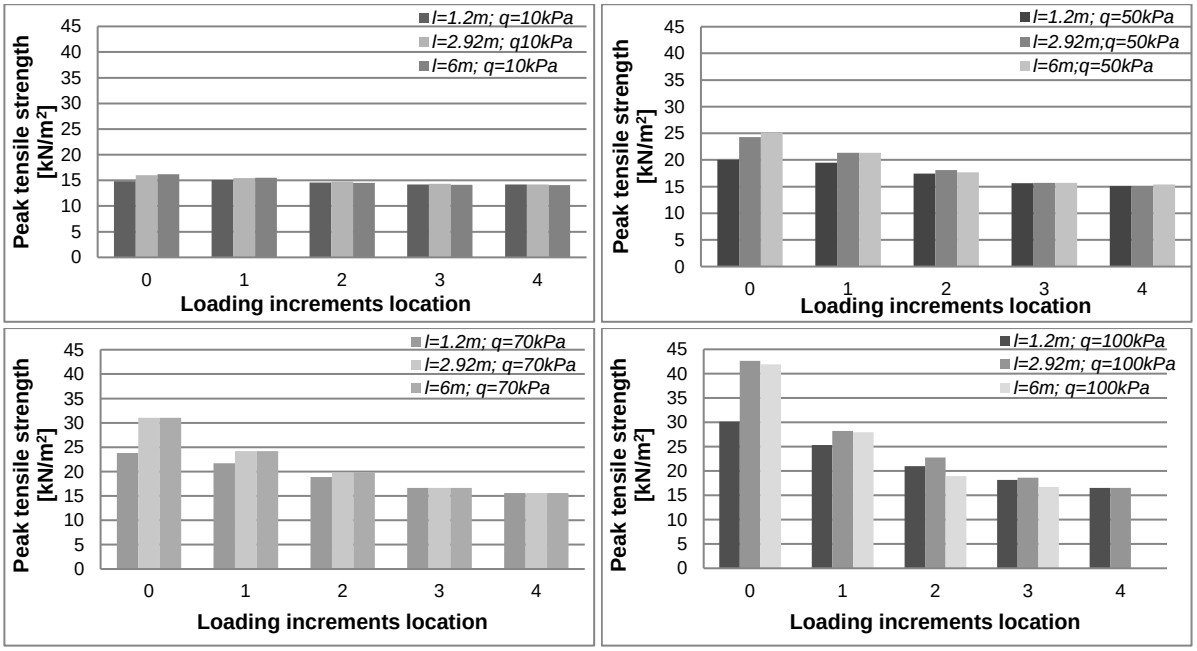
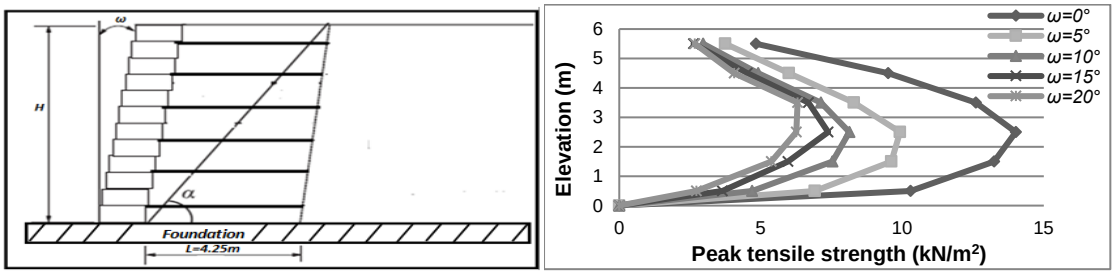


Fig. 10: Column charts of loading increment location for different loading width.

3.6 Effect of facing inclination angle *ω*

The facing inclination angle *ω* is one factor that changes the response of geogrid-reinforced retaining wall. In order evaluate the effect of this latter, the analyses were performed considering four values of *ω* = 5°, 10°, 15°, 20°.



a) b)

Fig. 11: a) Location of internal failure surface. b) Influence of facing inclination angle on peak tensile strength.

Fig. 11b shows that as the inclination angle decreases, the magnitude of peak tensile strength at each elevation increases also. These results can be justified by the reduction in the earth pressure coefficient k_a which was computed using Coulomb's theory that accounts for the effect of the facing inclination angle and soil-facing friction ratio. Also, the shape of the distribution of maximum tensile strength with depth was considered to be trapezoidal rather than linear, as assumed by earth pressure theory according to equation 2 recommended by the AASHTO design method.

$$T_{max} = k_a\,(\gamma H + q) S_v \tag{2}$$

Where:
ɣ - unit weight of soil,
H - wall height,
S_v - vertical spacing of geogrid,
q - loading increments.

The earth pressure coefficient was calculated using equation (3) (Rankine theory for vertical facing).

$$k_a = \tan^2\left(\frac{\pi}{4} - \frac{\varphi}{2}\right) \tag{3}$$

For inclined facing, the earth pressure coefficient was calculated by Coulomb theory using equation (4).

$$k_a = \frac{\cos^2(\varphi+\omega)}{\cos^2\omega\cos(\delta-\omega)\left[1+\sqrt{\frac{\sin(\varphi+\delta)\sin\varphi}{\cos(\delta-\omega)\cos\omega}}\right]^2} \tag{4}$$

Where:
φ - friction angle,
ω - facing inclination angle,
δ - soil-facing friction ratio.

AASHTO conception method [1] assumes that the location of peak tensile strength in each geogrid layer represents the internal failure surface. It should be noted that many of the experimental research and modeling work were consistent with the AASHTO design method [2, 4, 6, 7, 18]. The orientation of the internal failure surface, α can be calculated as a function of the failure line geometry, along the Rankine's theory for vertical facing wall (equation 5), and along the Coulomb's theory given by equation (6) for reinforced retaining inclined wall with *ω* ≥ 10°.

$$\alpha = \frac{\pi}{4} + \frac{\varphi}{2} \tag{5}$$

$$\tan(\alpha_\varphi) = \frac{-\tan\varphi + \sqrt{\tan\varphi[(\tan\varphi+\cot(\varphi+\omega))(1+\tan(\delta-\omega)\cot(\varphi+\omega)]}}{1+\tan(\delta-\omega)(\tan\varphi+\cot(\varphi+\omega))} \quad (6)$$

Where:
α - internal failure surface angle,
ϕ - friction angle,
ω - facing inclination angle,
δ - soil-facing friction ratio.

Fig. 12 illustrates the effect of facing inclination angle ω on the failure surface determined by the position of the peak tensile strength across the toe of the facing. For facing inclination angle greater than 10° from the vertical, the present study was in good agreement with the results greater than by [7, 17, 18], where the internal failure is parabolic. In addition, the failure surface was less than that predicted by the Rankine failure plane and it is close to that defined by Coulomb.

For facing inclination angle smaller than 10°, the critical failure surface was quasi-linear. The peak tensile strength farthest from wall was situated near Rankine's failure surface.

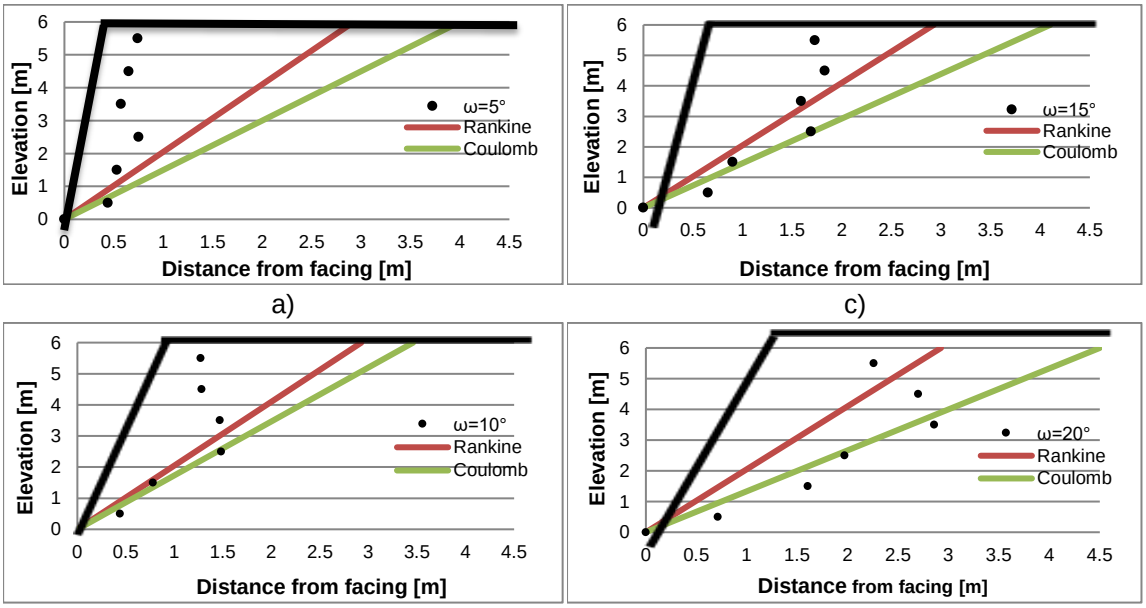


Fig. 12: Location of internal failure surface with: a) ω = 5°; b) ω = 10°; c) ω = 15°; d) ω = 20°.

3.7 Effect of geogrid inclination angle λ

The general consideration when choosing the effect of geogrid inclination angle λ was to be able to achieve the internal stability of the geogrid-reinforced soil retaining walls. Three different positions were examined as follows: λ = 0°, 5°, 10°.

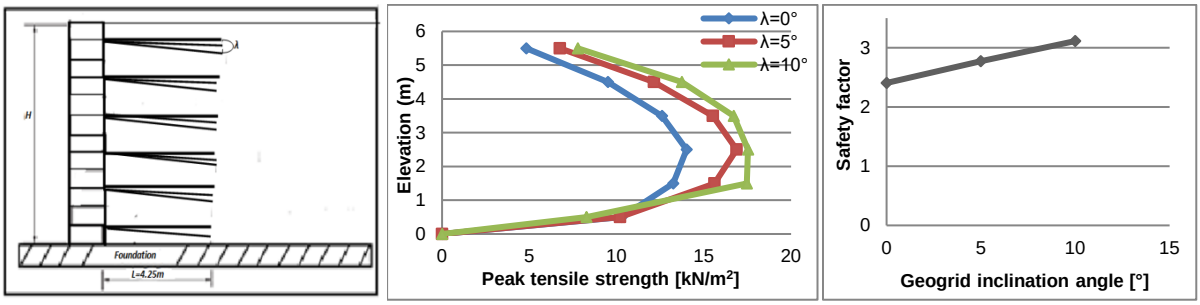
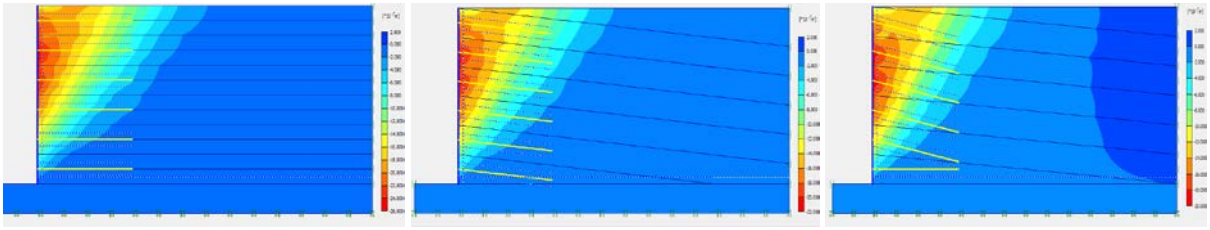


Fig. 13: a) Position of geogrid. b) Effect of the geogrid inclination angle on peak tensile strength. c) Safety factors.

The variation of the geogrid inclination angle of the peak tensile strength is presented in Fig. 13b). According to the curves trend, it can be distinguished that the peak tensile strength increases with increasing geogrid inclination angle and it was obtained at the mid-height of the reinforced zone. The peak tensile strength distribution becomes trapezoidal in shape. However, the influence of the geogrid inclination angle on the peak tensile strength was relatively small at the base of the reinforced retaining wall, due to the foundation stiffness.

The safety factor value was given as a function of geogrid inclination angle, as illustrated in Fig. 13c. It can be seen that the safety factor increases with the inclination angle of the geogrid.



Horizontal displacements (Max) - 25.72mm a)

Horizontal displacements (Max) - 21.36mm b)

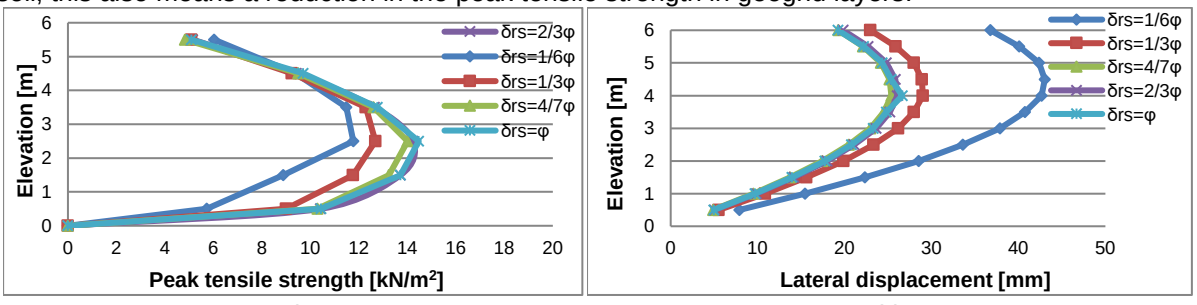
Horizontal displacements (Max) - 19.65mm c)

Fig. 14: Effect of geogrid inclination angle on lateral facing displacement: a) λ = 0°; b) λ = 5°; c) λ = 10°.

It can be inferred from Fig. 14, that the lateral facing displacements decrease with increasing the geogrid inclination angle, and it concentrates on the third upper part of the wall about 2 m from crest, and the geogrid-reinforced soil retaining wall fails internally. Considering the results, it could be concluded that the geogrid inclination angle has a major effect on the lateral facing displacements.

3.8 Effect of geogrid-soil friction factor δ_{rs}

To evaluate the effect of geogrid-soil friction factor δ_{rs} on the behavior of reinforced soil retaining wall with a segmental facing, some numerical analyses were carried out with different values: δ_{rs} =1/6φ, 1/3φ, 4/7φ, 2/3φ, φ corresponding to Fig.15a, b, the geogrid-soil friction factor δ_{rs} does not appear to have any significant effect on the behavior of reinforced soil retaining wall for values δ_{rs} greater than 0.6φ. In this case the critical value of δ_{rs} was in the order of 0.6φ. It is important to notice that this conclusion seems to be in accordance with the results obtained by some authors such as [11], concerning the relationship between the reinforcement -soil friction factor and peak tensile strength is almost unique for values δ_{rs} greater than 2/3φ. In addition, the friction factor required for calculating the minimum length of reinforcement layers recommended by AASHTO (2012) [1] is equal to 0.67tanφ.
For δ_{rs} less than 0.6φ, the lateral facing displacement increases due to sliding between the geogrid and soil, this also means a reduction in the peak tensile strength in geogrid layers.



a) b)

Fig. 15: Effect of the geogrid-soil friction factor on: a) Peak tensile strength. b) Lateral facing displacement.

4 Conclusion

The objective of this study is carried out to modeling the geogrid-reinforced soil retaining wall, using the finite element method with PLAXIS^{2D} [12] code, in order to understand the behavior of this structure, and to evaluate the influence of some geometrical and mechanical parameters, especially on the peak tensile strength in the geogrid layers, and on the lateral displacement of the wall. For the

validation of our numerical model, the results obtained in this research are compared to those obtained by [4, 6, 15]. The following conclusions may be drawn:

• Facing panel type does not affect maximum tensile strength in geogrid layers and numerically defined lateral displacement of facing (continuous or segmented) which remains close.

• The mobilization of peak tensile strength increases proportionally with loading increments. Also, the distribution of peak tensile strength was quasi-linear at high loading increments q ≥ 50 kPa and trapezoidal at low loading increments q < 50 kPa.

• The critical value of peak tensile strength was located at approximately the mid-height above the base of the wall 0.5*H*. This examination does not follow the triangular distribution with depth assumed in geogrid-reinforced retaining wall conception methodologies.

• The peak tensile strength and the lateral facing displacement are not dependent on the loading increments width beyond 0.5*H*, which coincides with the Ranking failure surface.

• The position of the peak tensile strength mobilized along the reinforcement layers may depend on the loading increment and the different loading increments locations. Due to the application of increasing loading increment towards the back of the facing, the position of the peak tensile strength may shift towards the soil reinforcement. This means that the location of the surcharge and the loading values can change the position of the maximum tension mobilized along the geogrid from a position closer to the facing to the soil reinforcement. The loading increments location can change the shape and the position of the peak tensile strength, which is more pronounced for the higher loading values.

• The AASHTO conception method overestimating the length of reinforcement layer has been proposed as a function of the failure line geometry.

• The present study is in agreement with the AASHTO conception method according to which the failure surface, was based on the Rankine plane for a vertical facing and the Coulomb plane with an inclined facing $\omega \geq 10°$.

• The geogrid inclination angle has a major effect on the lateral facing displacements and safety factor, the lateral displacements decrease with increasing geogrid inclination angle and the critical mechanical failure model was generally the internal failure given by PLAXIS^{2D}.

• The soil-geogrid friction ratio is not considered to have a major effect on the peak tensile strength value for friction ratio greater than $4/7\varphi$. In this case, the critical value of δ_{rs} is in the order of 0.6φ. However, the AASHTO method [1] takes this parameter into account in the calculation of the minimum length of the resistant zone.

References

[1] AASHTO, LRFD bridge design specifications, customary U.S. unit 2012. American Association of State Highway and Transportation Officials, Washington, DC, USA, 2012.

[2] HO, S. K.: A Numerical Investigation into the Behaviour of Reinforced Soil Walls. Thesis, Unive. of Western at Ontario, London,1993, https://ir.lib.uwo.ca/digitizedtheses/2298.

[3] BATHURST, R. J. - HATAMI, K.: Seismic response analysis of a Geosynthetic-reinforced soil retaining wall. Geosynthetics International, Vol. 5, No. 1–2, 1998, pp. 127–166, doi: 10.1680/gein.5.0117.

[4] ROWE, K. - HO, K. S.: Continuous panel reinforced soil walls on rigid foundation. Journal of Geotechnical and Geoenvironmental Engineering, 10.1061/ASCE10900241,1997,123:10(912), 912–920.

[5] HAZA, E.: Geosynthetic reinforced structures, locally loaded at the head: experimentation and calculation method. These University of Joseph-Fourier – Grenoble I, France, 1997, https://tel.archives-ouvertes.fr/tel-00785909.

[6] WAFA, D. - MOHAMED, S. - SOUHILA, A.: Numerical study of the behaviour of geosynthetic-reinforced soil retaining walls under a uniform surcharge. International Journal of Structural Engineering, Vol. 10, No. 2–2, 2020, pp. 139–149, https://doi.org/10.1504/IJSTRUCTE.2020.105632.

[7] OUASSIM, R. - MABROUKI, A. - BENMEDDOUR, D. - MELLAS, M.: A numerical investigation into the behavior of geosynthetic-reinforced soil segmental retaining walls. International Journal of Geotechnical Engineering, Vol. 10, No. 5, 2016, pp. 435–444, http://dx.doi.org/10.1080/19386362.2016.1158443.

[8] YANG, K. H. - UTOMO, P. - LIU, T. L.: Evaluation of force-equilibrium and deformation based design approaches for predicting reinforcement loads within geosynthetic reinforced soil structures. Journal of GeoEngineering, 8, (2), 2013, 41–54.

[9] LABOUDI, K. - RAHMOUNI, O. - LABED, M.: Numerical and Analytical Analysis of the Surcharge Application Distance influence on the Behavior of Reinforced Soil Retaining Wall. Indian Geotech J, 2022, https://doi.org/10.1007/s40098-022-00680-6.
[10] MARIANO, L. R. - MIRMORAD, S. H. - EHRLICH, M.: Evaluation of the effect of surcharge on the behavior of geosynthetic-reinforced soil walls. Transportation Geotechnics Journal, Vol. 31, 100634, 2021, https://doi.org/10.1016/j.trgeo.2021.100634.
[11] MIRMORADI, S. H. - EHRLICH, M.: Experimental evaluation of the effects of surcharge width and location on geosynthetic-reinforced soil walls. International Journal of Physical Modelling in Geotechnics, Vol, 19, Iss. 1, 2019, pp. 27-36, https://doi.org/10.1680/jphmg.16.00074.
[12] SULOVSKA, M. - STACHO, J.: Analysis of geogrid reinforced structures with a passive facing system using different computational methods. Civil and Environmental Engineering, Vol. 17, Iss. 2, 2021, pp. 500-512, doi: https://doi.org/10.2478/cee-2021-0052.
[13] Plaxis 2D: Plaxis finite element code for soil and rock analysis manual. Delft University of Technology and Plaxis, Delft, the Netherlands, 2004.
[14] YANG, K. H. - ZORNBERG, J. G. - LIU, C. N. - LIN, H. D.: Stress distribution and development within geosynthetic-reinforced soil slopes. Geosynthetics International, 19(1), 2012, 62-78, https://doi:10.1680/gein.2012.19.1.62.
[15] VIEIRA, C. S. - LOPES, M. L. - CALDEIRA, L. M.: Influence of facing panel rigidity on performance of reinforced soil retaining walls: a numerical study. Proceedings of the 4th european geosynthetics conference, 2008, 244 p., Edimburg.
[16] ZORNBERG, J. G. - ARRIAGA, F.: Strain distribution within geosynthetic-reinforced slopes. Journal of Geotechnical and Geoenvironmental Engineering, ASCE, 131, No. 2, 2003, 141–150.
[17] WOODRUFF, R.: Centrifuge Modeling of MSE-Shoring Composite Walls. Thesis, University of Colorado, Boulder, 2003.
[18] YANG, K. H. - ZORNBERG, J. G. - HUNG, W. Y. - LAWSON, C. R.: Location of Failure Plane and Design Considerations for Narrow GRS Wall Systems. Journal of Geo Engineering, Vol. 6, No. 1, April, 2011, pp. 27-40.